Spatially-Varying Calibration of Along-Track Monopulse Synthetic Aperture Radar Imagery for Ground Moving Target Indication and Tracking

Uttam Majumder[1], Mehrdad Soumekh[2], Michael Minardi[1], John Kirk[3]

1: Air Force Research Laboratory, 2241 Avionics Circle. Wright-Patterson AFB, OH 45433

2: Soumekh Consulting, Bethesda, Maryland, 20817

3: Goleta Star LLC. 24085 Garnier Street. Torrance, CA 90505

***Abstract*— In this research, we have developed an algorithm to reduce the residual artifacts of the background clutter (that is, stationary targets) that appear in the MTI imagery that are generated by Global Signal Subspace Difference (GSSD) of the monostatic and bistatic images of an along-track monopulse synthetic aperture radar (SAR) data. We have also established the theoretical foundation for estimating the motion track and parameters of the detected moving targets. We will show the results of these algorithms on measured SAR data.**

I. INTRODUCTION

In recent years, the United States Air Force Research Laboratory at Wright Patterson Air Force base has conducted nonlinear SAR data collections with an X-band radar system [1][5]. This platform is capable of making bistatic measurements in the along-track domain as well as monostatic measurements. The data were collected over an urban area that contained high stationary clutter (buildings, vegetation, etc.). The radiated scene also included various roads with different types of moving vehicles.

Due to the heavy clutter in the imaging scene, the signatures of most the moving targets fall below the clutter signature. We have developed a nonlinear subaperture-based coherent processing of dual receiver channels of the Gotcha platform to detect the moving targets [4]. This approach utilizes the 2D adaptive processing that we proposed in [2]-[4] to blindly calibrate the two receiver channels of an along-track monopulse SAR system. Furthermore, a pre-processing of the nonlinear subaperture data ensures the two channels are coherently calibrated with respect to the variations of the flight path. The current paper is concerned with calibration of the two along-track monopulse SAR images via a *global spatially-varying 2D adaptive filter* that provides more accurate information not only for ground moving target indication (GMTI) but also tracking data that could be exploited to estimate the motion parameters of a moving target. The basic principle behind extracting moving target indication (MTI) from two monostatic and bistatic along-track receiver channels of a SAR platform is that after compensating/calibrating for known deterministic differences of the two channels the SAR MTI image can be constructed via the following:

$$f_{MTI}(x,y) = f_m(x,y) - f_b(x,y),$$

where $f_m(x,y)$ and $f_b(x,y)$ are, respectively the monostatic and deterministically-calibrated monostatic and bistatic SAR images. In practice, due to unknown variations of the electronics, antennas, etc. of the two receiver channels, there are unknown phase and gain variations in both range and Doppler domains that are unknown to the user. The simplest way to model this is to assume that these variations are invariant in range and Doppler. In that case, under the null hypothesis that is there is no moving target, the monostatic and bistatic images are related via the following:

$$\begin{aligned} f_m(x,y) &= f_b(x,y) \otimes h(x,y) \\ &= \int f_b(x-u, y-v)\ h(u,v)\, du\, dv \end{aligned}$$

where $\otimes$ represents two-dimensional convolution, and $h(x,y)$ is an unknown two-dimensional filter. Under the null hypothesis, this filter can be determined using the least mean square (LMS) algorithm; this approach is called *adaptive filtering*. A practical implementation of this method for the two-dimensional problems was described in our previous work [2]-[4], and was referred to as Signal Subspace Processing (SSP).

A more realistic miscalibration model for the two receiver channels is based on the fact that the filter is *spatially-varying*. In this case, the relationship between the monostatic and bistatic images can be expressed via the following:

Correspondence POC: Uttam Majumder, Uttam.majumder@wpafb.af.mil

978-1-4244-5813-4/10/$26.00 ©2010 IEEE

Report Documentation Page

Form Approved
OMB No. 0704-0188

1. REPORT DATE **MAY 2010**	2. REPORT TYPE	3. DATES COVERED **00-00-2010 to 00-00-2010**

4. TITLE AND SUBTITLE **Spatially-Varying Calibration of Along-Track Monopulse Synthetic Aperture Radar Imagery for Ground Moving Target Indication and Tracking**	5a. CONTRACT NUMBER 5b. GRANT NUMBER 5c. PROGRAM ELEMENT NUMBER
6. AUTHOR(S)	5d. PROJECT NUMBER 5e. TASK NUMBER 5f. WORK UNIT NUMBER
7. PERFORMING ORGANIZATION NAME(S) AND ADDRESS(ES) **Air Force Research Laboratory,2241 Avionics Circle,Wright-Patterson AFB,OH,45433**	8. PERFORMING ORGANIZATION REPORT NUMBER
9. SPONSORING/MONITORING AGENCY NAME(S) AND ADDRESS(ES)	10. SPONSOR/MONITOR'S ACRONYM(S) 11. SPONSOR/MONITOR'S REPORT NUMBER(S)

12. DISTRIBUTION/AVAILABILITY STATEMENT
Approved for public release; distribution unlimited

13. SUPPLEMENTARY NOTES
See also ADM002322. Presented at the 2010 IEEE International Radar Conference (9th) Held in Arlington, Virginia on 10-14 May 2010. Sponsored in part by the Navy.

14. ABSTRACT
In this research, we have developed an algorithm to reduce the residual artifacts of the background clutter (that is stationary targets) that appear in the MTI imagery that are generated by Global Signal Subspace Difference (GSSD) of the monostatic and bistatic images of an along-track monopulse synthetic aperture radar (SAR) data. We have also established the theoretical foundation for estimating the motion track and parameters of the detected moving targets. We will show the results of these algorithms on measured SAR data.

15. SUBJECT TERMS

16. SECURITY CLASSIFICATION OF:			17. LIMITATION OF ABSTRACT	18. NUMBER OF PAGES	19a. NAME OF RESPONSIBLE PERSON
a. REPORT **unclassified**	b. ABSTRACT **unclassified**	c. THIS PAGE **unclassified**	**Same as Report (SAR)**	**6**	

$$f_m(x,y) = \int f_b(x-u, y-v)\ h_{xy}(u,v)\, du\ dv$$

where in this model the filter $h_{xy}(u,v)$ varies with the spatial coordinates, that is, (x,y). While the above model is a more suitable one, however, it is computationally prohibitive to implement the LMS or SSP method for this scenario.

A practical alternative is to assume that the filter is approximately spatially-invariant within a small area in the spatial domain. In this case, we can divide the SAR scene into subpatches within which the filter can be approximated to be spatially-invariant. The resultant model is given by:

$$\begin{aligned} f_{m\ell}(x,y) &= f_{b\ell}(x,y) \otimes h_\ell(x,y) \\ &= \int f_{b\ell}(x-u, y-v)\ h_\ell(u,v)\, du\ dv \end{aligned}$$

where ℓ represent an index for the subpatches.

In the approach that we call Local Signal Subspace Processing (LSSP), the LMS/SSP method is used to estimate the local unknown calibration filter $h_\ell(x,y)$. After this filter is estimated for each subpatch, an approach that we call Global Signal Subspace Processing (GSSP) is used to estimate the original spatially-varying filter $h_{xy}(u,v)$.

II. Mathematical Prelimenaries

The basic foundation of our work is the use of ***subaperture processing*** to not only detect but also geolocate and track moving targets. The simple and most prominent rational for exploiting subaperture processing is that the signature of a moving target appears fairly ***localized*** in subaperture SAR imagery though it is slightly smeared (Note that the signature of a moving target in a full-aperture image appears as a severely smeared structure in the formed image.). We should, however, point out that the subaperture image of a moving target may not be visible in the formed image. In fact, the ***coherent*** processing of the monostatic and bistatic images is the key in suppressing the background clutter and revealing the signature of the moving targets in the imaging scene.

We should also point out that subaperture processing has also merits in the case of SAR data that are collected over a ***nonlinear*** flight path. The reason for this is not just for imaging purposes for wavefront reconstruction. It turns out that a nonlinear subapertures that result in interrogating (imaging) the scene at different slant planes actually adds to the information base that is exploited to estimate the parameters of a moving target. This will be discussed later.

This section is intended to outline the basic equations that model the signature of a moving target in a subaperture. This model is the foundation of our approach to geolocate and track moving targets. We denote the slow-time domain with τ. We divided the SAR data into subapertures that overlap. The size of a subaperture is chosen such that the basic assumption that the subaperture image of a moving target is relatively localized. This, clearly, depends on the SAR system parameters (frequency band, platform speed, etc.) and the anticipated maximum speed of the ground moving targets. In the case of the Gotcha platform, a suitable subaperture size is about 1,204 PRIs. In our implementation, we use 512 PRIs for the overlap region between two adjacent subapertures.

Consider the ℓ-th subaperture of the flight path. In the subaperture wavefront processing, a spatially-varying motion compensation is used to convert the measured data over the nonlinear path every subaperture into a ***conventional linear SAR with a constant platform velocity*** for that subaperture; we call this the ***synthesized*** linear SAR subaperture. (We should emphasize that this approach motion compensates the measured SAR data for every individual point in the 3D spatial domain; that is, it is as accurate as the backprojection imaging.) We denote the radar coordinates at the midpoint of the resultant linear SAR for the ℓ-th subaperture by

$$\left(X_{\text{radar}}^{(\ell)}, Y_{\text{radar}}^{(\ell)}, Z_{\text{radar}}^{(\ell)}\right)$$

We also denote the constant velocity of the synthesized linear SAR subaperture by

$$\left(v_{\text{xradar}}^{(\ell)}, v_{\text{yradar}}^{(\ell)}, v_{\text{zradar}}^{(\ell)}\right)$$

Note that the synthesized platform velocity does vary from one subaperture to another.

Next, we identify the slant-plane where the image is formed for the ℓ-th subaperture. We denote the 3D spatial domain by (x,y,z). (This is equivalent to what is called PCS coordinate system by General Dynamics.) The wavefront processor forms a slant-plane image with motion compensation that incorporates variations in terrain (using Digital Elevation Map, DEM). The final output of the wavefront processor is a 2D image on the (x,y) plane that is interpolated from the slant-plane SAR image. For convenience, we refer to the 2D ground (x,y) domain as the ***UTM domain*** (though the true UTM domain is a rotated version of the PCS coordinate system); we also call the two variables (x,y) as the ***Northing*** and ***Easting*** coordinates; this terminology is used to identify the UTM domain.

The slant-plane where the image is formed is denoted with (x_s, y_s) where slant-plane range,

$$x_s = \sqrt{x_{gs}^2 + \left(Z_{\text{radar}}^{(\ell)} - Z_{\text{target}}\right)^2} \qquad (1)$$

Slant-plane cross-range,

$$y_s = -x \sin\theta_\ell + y \cos\theta_\ell \qquad (2)$$

Slant-plane ground range,

$$x_{gs} = x \cos\theta_\ell + y \sin\theta_\ell \qquad (3)$$

Target area mean elevation is defined by Z_{target} and synthesized flight path motion angle is θ_ℓ.

We should point out that the 2D slant-plane (x_s, y_s) varies with each subaperture and should be denoted with $(x_s^{(\ell)}, y_s^{(\ell)})$. For notational simplicity, we drop the superscript ℓ to identify the 2D slant-plane. The wavefront processor produces two SAR images on the slant-plane using monostatic and bistatic data for each Subaperture. We denote these via $f_{\text{mono}}^{(\ell)}(x_s, y_s)$ and $f_{\text{bist}}^{(\ell)}(x_s, y_s)$. Furthermore, the coherent signal subspace processing of these two imagery results in the GSSD that is the MTI information; we define this by $f_{\text{MTI}}^{(\ell)}(x_s, y_s)$.

Using the inverse of the transformations in equations (1)-(3), these slant-plane images are transformed into the ground plane of the PCS coordinate system; we refer these as

$$f_{\text{mono}}^{(\ell)}(x_s, y_s) \Rightarrow g_{\text{mono}}^{(\ell)}(x, y)$$
$$f_{\text{MTI}}^{(\ell)}(x_s, y_s) \Rightarrow g_{\text{MTI}}^{(\ell)}(x, y)$$

III. RESIDUAL CLUTTER SIGNATURE SUPPRESSION

The coherent signal subspace processing yields an MTI information base $f_{\text{MTI}}^{(\ell)}(x_s, y_s)$ in which the background clutter is ***mostly*** suppressed. This slant-plane image, however, does contain some residual clutter signature. Since the slant-planes vary with each subaperture, the residual clutter signatures do not appear at the same coordinates in the subaperture images (though they correspond to the effects of ***stationary*** targets). Meanwhile, when the subaperture MTI images are transformed into the UTM domain, that is, $g_{\text{MTI}}^{(\ell)}(x, y)$ the transformed residual clutter signatures do co-register in the UTM coordinates.

This property can be exploited to further reduce the clutter signature in the UTM domain MTI imagery. For this purpose, we construct a ***reference image*** via a subaperture ℓ domain median filtering of the MTI images for every point in the UTM coordinates. We denote the resultant by $g_{\text{ref}}(x, y)$. This image is basically a representative of the ***common*** residual clutter signature in all the MTI imagery; it contains almost no moving target signature. Next, we use this reference image in the adaptive filtering method of signal subspace processing to reduce the residual clutter signature in each subaperture MTI image $g_{\text{MTI}}^{(\ell)}(x, y)$. We denote the final MTI image by $g_{\text{MTI-R}}^{(\ell)}(x, y)$.

IV. MOVING TARGET SIGNAL MODEL AND IMAGE SIGNATURE WITHIN A SUBAPERTURE

Our next task is to examine the issues that are associated with tracking a detected moving target and estimating its motion parameters. To do so, we first develop a signal model for the signature of a moving target and its image signature within a subaperture. In our model, we assume the velocity of a moving target is constant within a single subaperture. Consider a moving target that is located at the coordinates

$$(X_{\text{target}}, Y_{\text{target}}, Z_{\text{target}})$$

at the slow-time $\tau = 0$, that is, at the midpoint of the subaperture. Furthermore, the 3D velocity of this moving target is denoted with

$$(v_{x\text{target}}, v_{y\text{target}}, v_{z\text{target}})$$

Thus, the radial distance of the target from the radar as a function of the slow-time is

$$R_{\text{radar-target}}^{(\ell)}(\tau) = \begin{bmatrix} \left(X_{\text{radar}}^{(\ell)} + v_{x\text{radar}}^{(\ell)}\tau - X_{\text{target}} - v_{x\text{target}}\tau\right)^2 + \\ \left(Y_{\text{radar}}^{(\ell)} + v_{y\text{radar}}^{(\ell)}\tau - Y_{\text{target}} - v_{y\text{target}}\tau\right)^2 + \\ \left(Z_{\text{radar}}^{(\ell)} + v_{z\text{radar}}^{(\ell)}\tau - Z_{\text{target}} - v_{z\text{target}}\tau\right)^2 \end{bmatrix}^{1/2} \tag{4}$$

We denote the ***angular Doppler frequency*** of this target via the following: $\phi_{\text{radar-target}}^{(\ell)}(\tau)$.

Using SAR signal theory, the radar-target distance and the angular Doppler frequency are related via the following:

$$\sin\phi_{\text{radar-target}}^{(\ell)}(\tau) = \frac{d}{d\tau} R_{\text{radar-target}}^{(\ell)}(\tau)$$
$$= \frac{\begin{bmatrix} \left(v_{x\text{radar}}^{(\ell)} - v_{x\text{target}}\right)\left(X_{\text{radar}}^{(\ell)} + v_{x\text{radar}}^{(\ell)}\tau - X_{\text{target}} - v_{x\text{target}}\tau\right) + \\ \left(v_{y\text{radar}}^{(\ell)} - v_{y\text{target}}\right)\left(Y_{\text{radar}}^{(\ell)} + v_{y\text{radar}}^{(\ell)}\tau - Y_{\text{target}} - v_{y\text{target}}\tau\right) + \\ \left(v_{z\text{radar}}^{(\ell)} - v_{z\text{target}}\right)\left(Z_{\text{radar}}^{(\ell)} + v_{z\text{radar}}^{(\ell)}\tau - Z_{\text{target}} - v_{z\text{target}}\tau\right) \end{bmatrix}}{R_{\text{radar-target}}^{(\ell)}(\tau)} \tag{5}$$

As we mentioned earlier, the principal assumption in our subaperture-based approach is that the signature of a moving target appears fairly localized in subaperture images. This location in the polar coordinates of the slant-plane are the radar-target radial distance and the angular Doppler frequency at the midpoint of the subaperture (that is, the slow-time $\tau = 0$):

$$\left[\phi_{\text{radar-target}}^{(\ell)}(0), R_{\text{radar-target}}^{(\ell)}(0)\right] \tag{6}$$

Thus, the slant-plane coordinates of the moving target in the subaperture images are

$$x_{s\text{target}}^{(\ell)} = R_{\text{radar-target}}^{(\ell)}(0)\cos\phi_{\text{radar-target}}^{(\ell)}(0)$$
$$y_{s\text{target}}^{(\ell)} = R_{\text{radar-target}}^{(\ell)}(0)\sin\phi_{\text{radar-target}}^{(\ell)}(0)$$

Using the mapping from the slant-plane to the UTM domain, the slant-plane coordinates of the moving target can be converted to its ground UTM (PCS) coordinates:

$$\left[x^{(\ell)}_{\text{starget}}, y^{(\ell)}_{\text{starget}}\right] \quad \Rightarrow \quad \left[x^{(\ell)}_{\text{target}}, y^{(\ell)}_{\text{target}}\right]$$

The distance of this signature from the location of the platform at the mid-point of the apertures in the UTM domain is:

$$\begin{aligned} R^{(\ell)}_{\text{target}} &= \sqrt{\left(X^{(\ell)}_{\text{radar}} - x^{(\ell)}_{\text{target}}\right)^2 + \left(Y^{(\ell)}_{\text{radar}} - y^{(\ell)}_{\text{target}}\right)^2} \\ &= \sqrt{\left[R^{(\ell)}_{\text{radar-target}}(0)\right]^2 - \left(Z^{(\ell)}_{\text{radar}} - Z_{\text{target}}\right)^2} \end{aligned}$$

V. Results

The overall signal processing used in our approach is shown in Figures 1 and 2. Figure 3 is the UTM domain reconstruction of the interrogated for Subaperture 1. Figure 4 shows the MTI image for the same scene using the coherent GSSP.

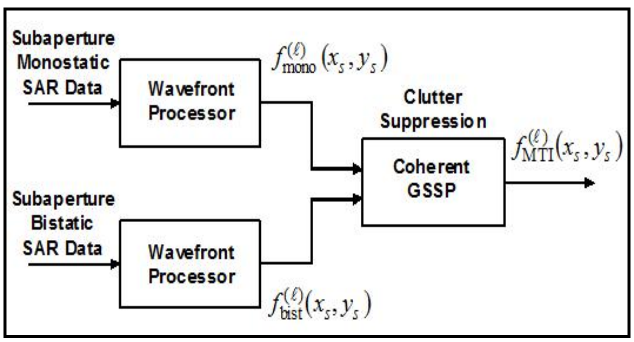

Figure 1. Wavefront Reconstruction and Coherent Clutter Suppression with Monostatic and Bistatic Data of Along-Track Monopulse SAR

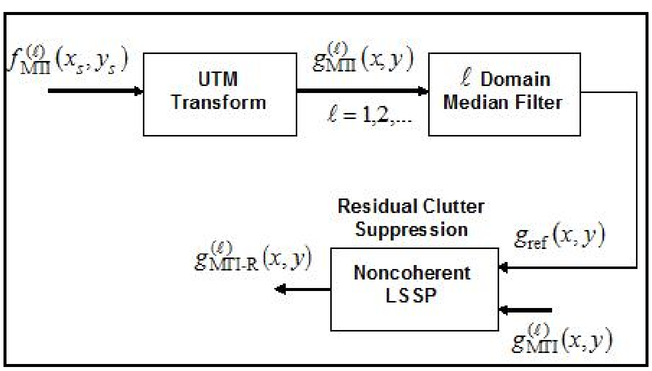

Figure 2: Slant-Plane to UTM (Ground-Plane) Transformation of MTI Image, and Residual Clutter Suppression

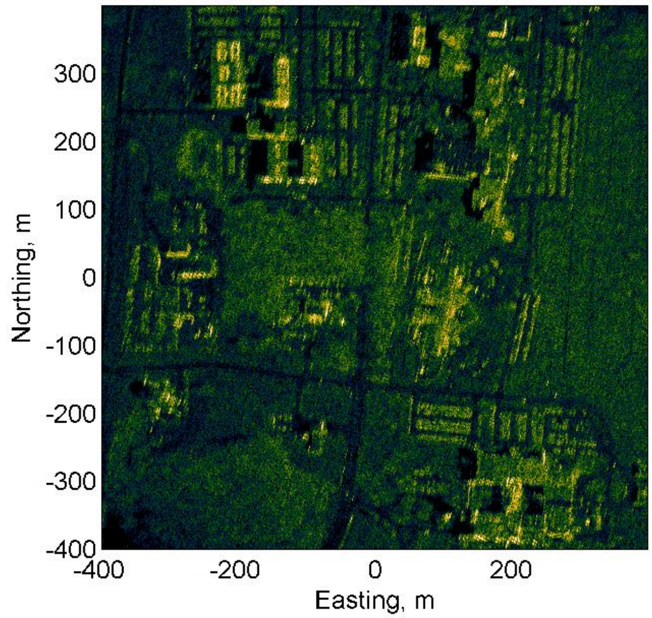

Figure 3: UTM Reconstruction: FP-128; Subaperture 1

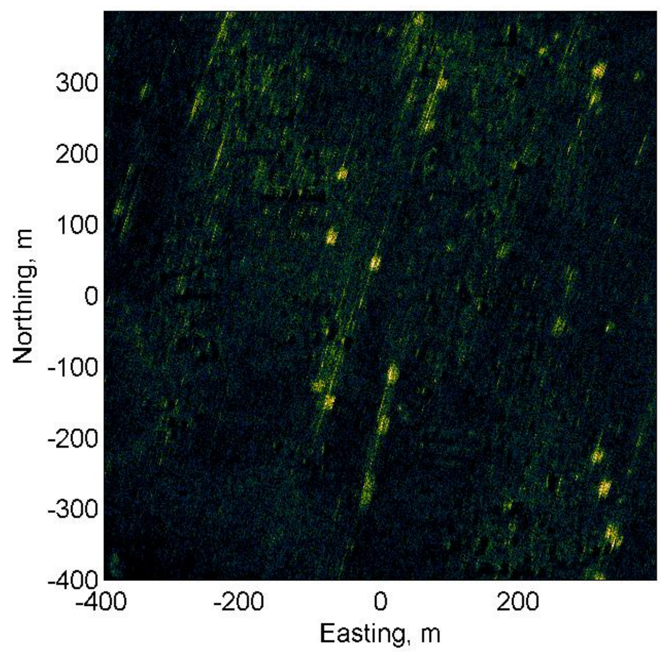

Figure 4: Coherent MTI via GSSP in UTM Domain: FP-128; Subaperture 1

Figure 5 is the reference image that is constructed from the median filtering of the UTM domain MTI-GSSD imagery; see the block diagram in Figure 2. Figure 6 is the resultant MTI image for Subaperture 1 using non-coherent LSSP processing of the MTI-GSSD image of Figure 6 and the reference image of Figure 5. We have generated movies of these results for a set of the subaperture.

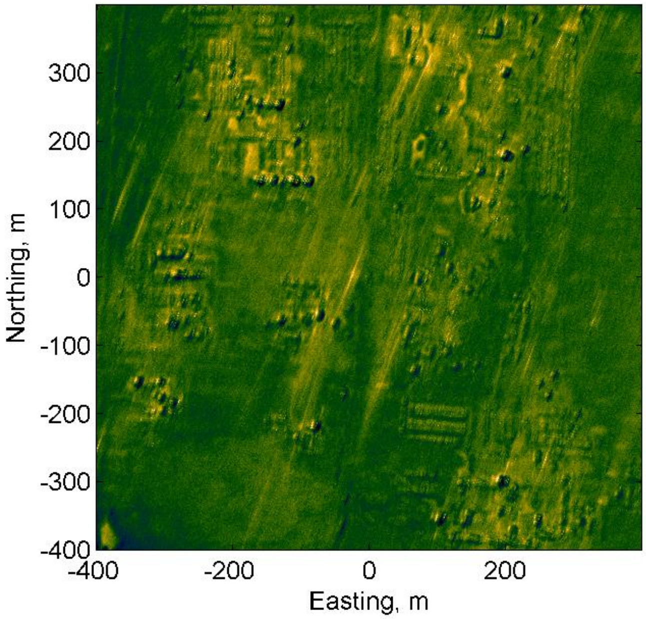

Figure 5: Reference Image Used for Residual Clutter Suppression

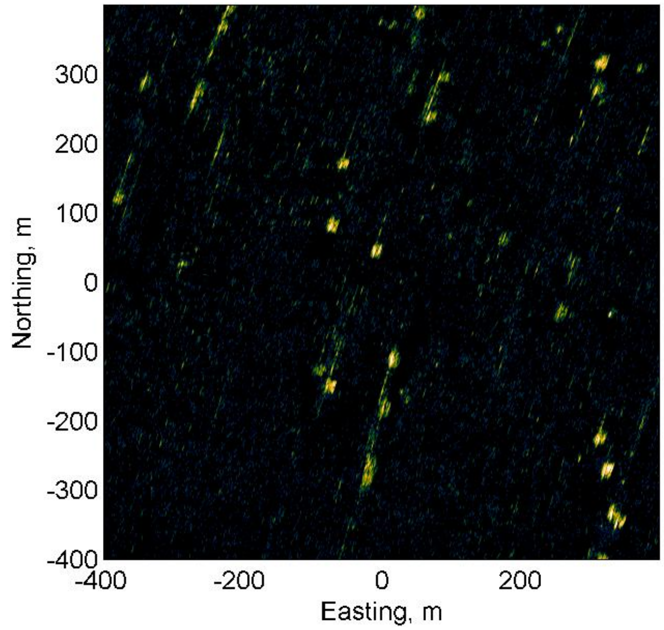

Figure 6: MTI After Residual Clutter Suppression
FP-128; Subaperture 1

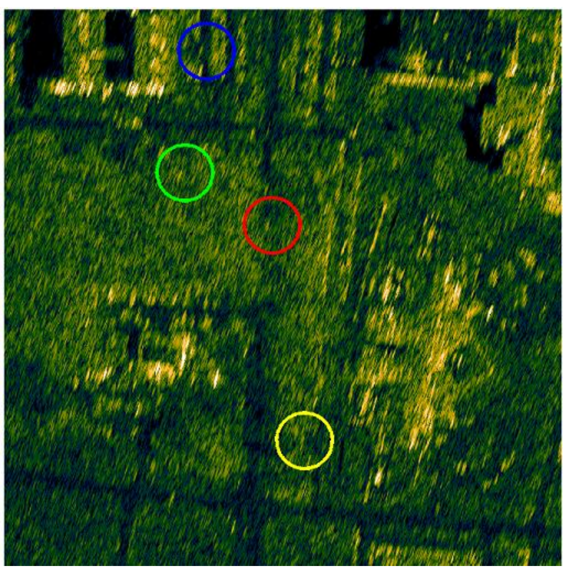

Figure 7a: Detected Moving Targets in Reconstruction and MTI. FP-128; Subaperture 1

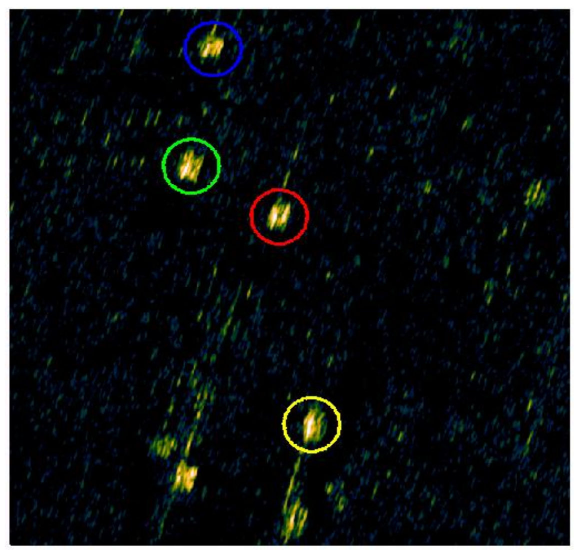

Figure 7b: Detected Moving Targets in Reconstruction and MTI. FP-128; Subaperture 1 (zoomed version)

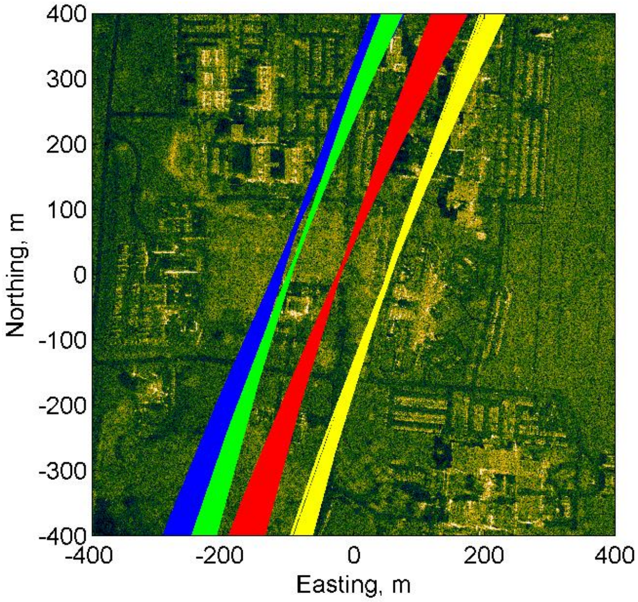

Figure 8a: Radial Locations of Detected Moving Targets

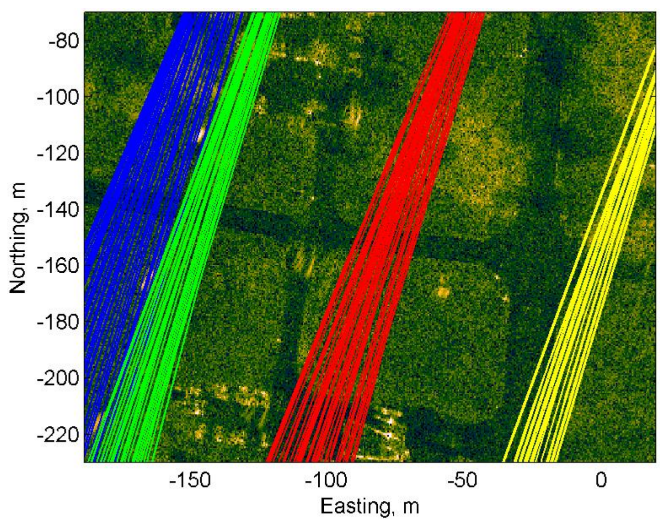

Figure 8b: Radial Locations of Detected Moving Targets (zoomed version)

VI. CONCLUSION

In this paper, we have presented an algorithm to reduce the residual artifacts of the background clutter that appear in the MTI imagery. This was accomplished by Global Signal Subspace Difference (GSSD) of the monostatic and bistatic images of an along-track monopulse SAR data. We have described the theoretical foundation for estimating the motion track and parameters of the detected moving targets. The results presented here were generated using Gotcha radar data. This research will continue to detect, geolocate and tracking multiple moving targets in SAR imagery in real-time.

ACKNOWLEDGMENT

The authors would like to thank Mr. LeRoy Gorham for description of the Gotcha data, Mr. Steven Scarborough and Mr. Edmund Zelnio for valuable technical discussions on the merit of this algorithm.

REFERENCES

[1] U. Majumder, M. Minardi, E. Blasch, L. Gorham, K. Naidu, T. Lewis and R. Williams, “Radar Signals Dismount Data Production,” *Proc. SPIE Defense and Security Conference*, Orlando, April 2006.

[2] M. Soumekh, “Signal Subspace Fusion of Uncalibrated Sensors with Application in SAR and Diagnostic Medicine,” *IEEE Transactions on Image Processing*, vol. 8, no. 1, pp. 127-137, January 1999.

[3] M. Soumekh, “Moving Target Detection and Imaging Using an X Band Along-Track Monopulse SAR,” *IEEE Transactions on Aerospace and Electronic Systems*, vol. 38, no. 1, pp. 315-333, January 2002.

[4] U. Majumder, et. al, “SAR-MTI Processing of Along-Track Monopulse Nonlinear SAR GOTCHA Data,” *Proc. IEEE Radar Conference*, Pasadena, May 2009.

[5] S. Scarborough, C. Casteel, Jr., L. Gorham, M. Minardi, U. Majumder, M. Judge, E. Zelnio, M. Bryant, H. Nichols, and D. Page, “A Challenge Problem for SAR-based GMTI in Urban Environments”, Proc. SPIE, Vol. 7337, 73370G (2009)